*Journal of Mining and Metallurgy, 39 (1–2) B (2003) 383 - 405.*

# EQUILIBRIUM ELECTROCHEMICAL SYNTHESIS DIAGRAMS OF SYSTEMS, FORMING HOMOGENEOUS ALLOYS AND COMPOUNDS

**G.Kaptay**

University of Miskolc, Department of Physical Chemistry
Hungary, 3515 Miskolc, Egyetemvaros
kaptay@hotmail.com

*(Received 20 January 2003; accepted 2 February 2003)*

## Abstract

*In the present paper thermodynamic limitations will be derived and summarized in the form of Equilibrium Electrochemical Synthesis (EES) diagrams, in order to predict the composition of the equilibrium phase, synthesized by galvanostatic co-deposition of components on inert electrodes. As a thermodynamic parameter, a difference of deposition potentials of pure components (ΔE) on inert cathodes is used (this parameter is a function of melt composition and temperature). Generally, the EES diagram predicts the equilibrium composition of the alloy as function temperature and ΔE. However, for systems with homogeneous alloy formation the composition-ΔE diagrams, drawn at a fixed temperature are more informative. As examples, EES diagrams are constructed for the liquid Mg-Nd alloy, for some A(III)-B(V) (where A = Al, Ga, In and B = As, Sb), Si-C and for the Al-Ti system. For the Al-rich part of the Al-Ti system, also a semi-schematic non-equilibrium ES diagram is constructed. Based on these diagrams, the synthesis conditions of various phases has been discussed.*

*Keywords:* electrochemical synthesis, ionic liquids, molten salts, phase diagrams, Mg-Nd, Si-C, A(III)-B(V), Ti-Al

## 1. Introduction

Electrochemical synthesis of alloys and compounds by co-depositing two, or

more components at an inert cathode is one of the promising ways to produce coatings or powders from molten salts and ionic liquids. Examples of this approach can be found in a large number of journal and conference proceedings papers, including those, published in this special issue [1]. The goal of electrochemical synthesis in the majority of cases is to produce one given phase with pre-defined composition. Electrochemical synthesis (ES) is usually performed in one of the following two ways:

a) **in a potentiostatic way**, i.e. at a given potential regarding a (stable) reference electrode. In principle, a certain value of the synthesis potential corresponds to each composition of the alloy. Similarly, a certain range of potentials corresponds to each possible compound, which is able to form from the co-deposited elements. However, in certain cases (especially for alloys) this range of potentials can be quite narrow. Therefore, potentiostatic synthesis can be successfully performed only, if a perfectly stable reference electrode is applied. However, the problem of stable reference electrodes is not routinely resolved, especially in high temperature molten salts, and so ES in a potentiostatic way cannot be always applied successfully.

b) **in a galvanostatic way**, i.e. at a given current. This way of ES is more convenient, as there is no need in a reference electrode, at all. However, controlling the current does not necessarily mean that one also controls the actual current density of ES. In reality, both electron conductivity of the electrolyte and the increasing surface area of the working electrode during the process might decrease the effective current density of ES. Nevertheless, at least the maximum current density during ES can be well controlled during galvanostatic synthesis.

In the present paper the principle to construct Equilibrium Electrochemical Synthesis (EES) diagrams is presented for ES of alloys and compounds, synthesized in a galvanostatic way on an inert cathode. This principle has been developed earlier by the Author for compounds with negligible homogenity range [2, 3] and was mainly applied for boride systems [2-6]. EES diagrams for the binary Ti-B system [2, 3], for all binary transition metal – boron systems [4], for the ternary Ti-Al-B system [5] and for the binary Al-Gd, La-B, Gd-B, and Al-La systems [6] have been already constructed. Kinetic limitations have also been included in our recent paper [7], on the example of the Ti-B system. In the present paper, the principle to construct EES diagrams is extended to homogeneous alloys. Several new EES diagrams will be constructed.

## 2. Thermodynamic basics of electrochemical synthesis

Let us consider an electrolyte, consisting of $A^{+n}$ and $B^{+m}$ ions, discharging at an inert cathode at potentials $E_A$ and $E_B$. Both of these quantities are functions of the electrolyte composition and temperature (and of-course pressure, but below 10 MPa its influence is negligible). Now, let a joint cathodic product of general composition $A_xB_{1-x}$ form at the cathode from the A and B ad-atoms, with a synthesis potential $E_S$. Then, the energy of the alloying or compound formation $\Delta G$ is spent on shifting the deposition potential of (1-x) moles of component B from $E_B$ to $E_S$, and on shifting the deposition potential of x moles of component A from $E_A$ to $E_S$. Hence, the following equation can be written:

$$-\Delta G = n \cdot x \cdot F \cdot (E_S - E_A) + m \cdot (1-x) \cdot F \cdot (E_S - E_B) \tag{1}$$

where: $\Delta G$ (kJ/g-atom) is the mixing Gibbs is energy of alloying for homogeneous alloys, while for compounds $A_pB_q$: $\Delta G = \Delta_f G^o_{ApBq}/(p + q)$, where $\Delta_f G^o_{ApBq}$ is the standard Gibbs energy of formation of the compound (kJ/mol),

x – mole fraction of component A in the homogeneous alloy; for compounds $A_pB_q$ (with p and q being integer numbers): $x = p/(p + q)$,

F is the Faraday number.

Introducing the potential difference $\Delta E = E_B - E_A$, the equilibrium synthesis potential $E_S$ can be expressed from the above equation, relative to the deposition potential of component A, as:

$$E_S - E_A = \frac{m \cdot (1-x)}{c} \cdot \Delta E - \frac{\Delta G}{c \cdot F} \tag{2}$$

where $c = n \cdot x + m \cdot (1-x)$.

In equilibrium (i.e. at very low current density values) the first cathodic product will be the one, having a most positive synthesis potential among all possible components, compounds or alloys to be synthesized. Eq.(2) can be used to find the value of x, corresponding to the most positive value of $(E_s - E_A)$, as function of $\Delta G$, $\Delta E$, m and n. Based on this principle, the desired EES diagrams can be constructed. EES diagrams will be constructed in the present paper for the following three limiting types of phase diagrams:

i. the case of homogeneous solid (or liquid) A-B solutions, with no compound formation and no limit of solubility,
ii. the case, when only one compound with practically no homogenity range is formed,
iii. the case, when several compounds with practically no homogenity range are formed.

It should be mentioned that some other algorithms have also been suggested in the literature to study thermodynamics of electrochemical synthesis of alloys [1.c, 8, 9]. One of the common ways to predict the composition of electrochemically co-deposited alloys is to suppose that the two components are deposited at the same potential due to their partial depolarization values [8, 9]:

$$E_A - \frac{\Delta G_A}{n \cdot F} = E_B - \frac{\Delta G_B}{m \cdot F} \tag{1.a}$$

where $\Delta G_A$ and $\Delta G_B$ (kJ/mol) are the partial mixing Gibbs energies of components.

From Eq.(1.a), taking into account our notation $\Delta E = E_B - E_A$, the following equation can be obtained:

$$\Delta E = \frac{\Delta G_B}{m \cdot F} - \frac{\Delta G_A}{n \cdot F} \tag{2.a}$$

If one applies Eq-s (2) or (2.a) for the given homogeneous alloy phase, the same equilibrium composition of the alloy can be computed, so the two methods are identical. As will be shown below, Eq.(2.a) is even more convenient for calculations, as the result can be obtained without iteration (at least for $\Delta E$ as function of x, but not for x as function of $\Delta E$ – see below).

However, Eq.(2.a) does not contain the synthesis potential, and so for systems, in which more than one phase can be formed, the most stable phase cannot be identified from Eq.(2.a) in a straightforward way. Also, for systems, containing compound phases, very often only limited thermodynamic information is known, such as the (integral) Gibbs energy of formation of some of the compound phases, from which the partial Gibbs energy values of the components do not follow in an easy way. That is why, for a general method to construct EES diagrams, Eq-s.(1-2) are preferred to Eq-s (1.a-2.a).

### 3. The EES diagram for a homogeneous alloy

When components A and B form no compounds, and are soluble in each other

without limitations at the given temperature (and pressure), the Gibbs energy of the alloy formation can be generally written:

$$\Delta G = \Delta G^{o} + \Delta G^{id} + \Delta G^{E} \tag{3}$$

where $\Delta G^{o}$ – is the average Gibbs energy of formation of the mixture of the two pure phases (if both phases have identical standard states, such as liquid, or fcc solid, etc, both of them can be taken as zero for the given T and p):

$$\Delta G^{o} = x \cdot \Delta_f G_A^{o} + (1-x) \cdot \Delta_f G_B^{o} \tag{3.a}$$

$\Delta G^{id}$ is the Gibbs energy of mixing of an ideal solution, which can be written, using the expression for the integral configurational entropy, as:

$$\Delta G^{id} = R \cdot T \cdot \left[ x \cdot \ln x + (1-x) \cdot \ln(1-x) \right] \tag{3.b}$$

where R = 8.314 J/molK, and T – is the absolute temperature (K),

$\Delta G^{E}$ is the excess Gibbs energy of mixing, which in a most simple case of a regular solution model can be written as:

$$\Delta G^{E} = \Omega \cdot x \cdot (1-x) \tag{3.c}$$

where Ω is a model parameter, describing the interaction between atoms A and B in the alloy.

Substituting Eq-s (3, 3.a-c) into Eq.(2), the synthesis potential can be calculated as function of temperature, alloy composition and parameter ΔE, if for the given system parameter Ω is known. As an example, in Fig.1 the dependence of the synthesis potential on the alloy composition is shown for different fixed values of T, Ω and ΔE, for pure phases, having identical standard states (i.e. $\Delta G^{o}$ = 0). In each figure 1.a-1.d three curves are shown, corresponding to ΔE = -10, 0 and +10 mV. The synthesis of an alloy of given composition will be thermodynamically favorable, if its synthesis potential will have the most positive value compared to all other compositions, including pure components A and B. Thus, from the maximum points of the curves, the equilibrium composition of the alloy can be found. The equilibrium composition of the alloy will be a function of T, Ω and ΔE. As the latter is the function of T and electrolyte composition, the equilibrium alloy composition will be finally a difficult function of the electrolyte composition, temperature and excess Gibbs energy of the alloy formation

1.a.

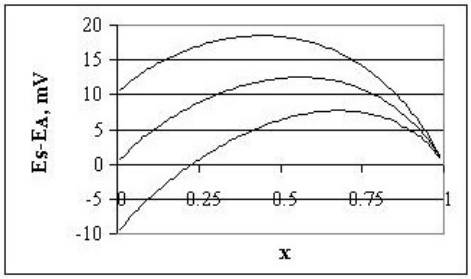


1.b.

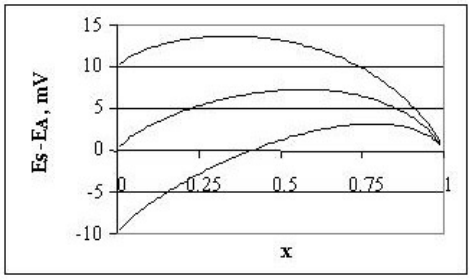


1.c.

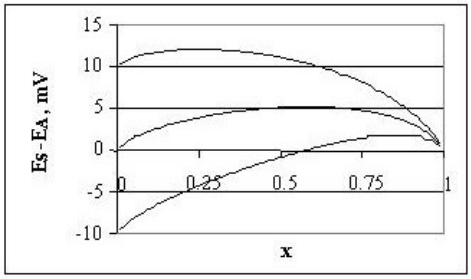


1.d.

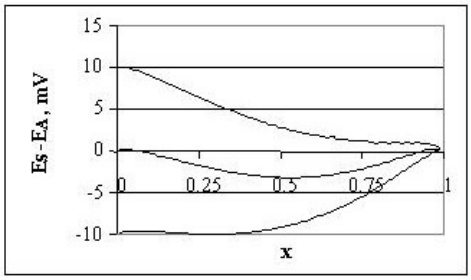


*Figure 1. The synthesis potential of the $A_xB_{1-x}$ alloy (relatively to the deposition potential of A) from an electrolyte containing $A^{+2}$ and $B^{+3}$ ions as function of the alloy composition at different values of $\Delta E$=-10 mV, 0 mV and +10 mV (for curves from bottom to top), at values of parameter $\Omega$=-5 kJ/mol (1.a), $\Omega$=0 kJ/mol (1.b), $\Omega$=+2 kJ/mol (1.c) and $\Omega$=+10 kJ/mol (1.d), at T=300 K.*

At the equilibrium alloy composition $E_s$ will have its maximum value. Unfortunately, this maximum value cannot be found analytically, as mixed x, lnx, x·lnx and $x^2$ terms appear after the derivation of Eq. (2), if Eq-s (3., 3.a-c) are substituted into it for ΔG. However, the solution can be obtained numerically. As an example, a result of such a numerical calculation is shown in Fig.2 for a system, containing $A^{+2}$ and $B^{+3}$ electrochemically active ions, as function of ΔE, at fixed values of T and Ω. Figures 2 are actually the EES diagrams for hypothetical $A^{+2}$ - $B^{+3}$ systems. On the top of Fig.2.c, the stability ranges of 'pure' A, the A-B alloy and 'pure' B are shown for T = 300 K. Let us mention the 'pure' A and 'pure' B means here only that the purity of these phases is above 99 %.

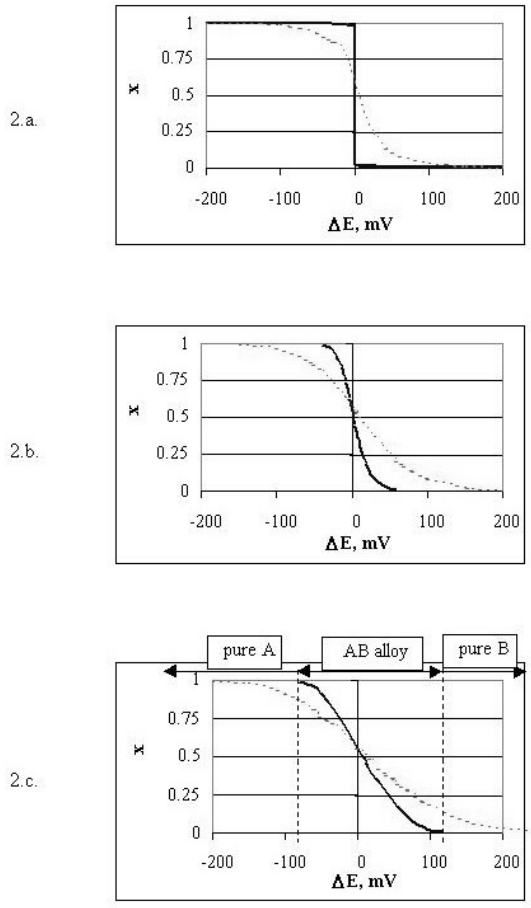


*Figure 2. Possible EES diagrams of the $A^{+2}$-$B^{+3}$ system calculated with Ω=+10 (2.a), Ω=0 (2.b) and Ω=-10 kJ/mol (2.c) at T=300 K (bold lines) and T=1,000 K (broken lines).*

Let us mention that Fig-s 2 (except the bold line in Fig.2.a – see below) can be drawn also without iteration, by applying Eq-s (2.a, 3.a-c), and also taking into account the relationship between integral and partial Gibbs energies of an alloy. For the simplified alloy model presented by Eq.(3.c), the following relationship can be obtained for ΔE:

$$\Delta E = \frac{R \cdot T}{F} \cdot \left[ \frac{ln(1-x)}{m} - \frac{ln\, x}{n} \right] + \frac{\Omega}{F} \cdot \left[ \frac{x^2}{m} - \frac{(1-x)^2}{n} \right] \qquad (2.b)$$

In Fig.2.b, the results for an ideal alloy are shown at two different temperatures. At ΔE = 0, x = 0.57 is obtained. Such an asymmetric result is a consequence of non-equal oxidation states of the electrochemical active ions, $A^{+2}$ and $B^{+3}$. As a general rule, at ΔE = 0 the alloy is more rich in a component, which has a lower oxidation state in the electrolyte. The same asymmetry remains in the whole range of ΔE values. When ΔE < 0, i.e. when the deposition potential of component A is more positive than that of B, the alloy gradually becomes more and more rich in A, and vice-versa. One can see that at higher temperature the potential window of alloy synthesis increases, due to the increasing role of the configurational entropy (see Eq.3.b).

From comparison of Fig-s 2.a-c one can see that the potential range of alloy formation also increases with more and more negative value of parameter Ω, due to the relative attraction of atoms A and B in the alloy. The more negative is the value of Ω, the less is the effect of temperature on the potential window of alloy formation, as the role of the configurational entropy in the total value of ΔG decreases.

It should be noted that a one-phase alloy will be formed only, if there is a total solubility in the corresponding A-B phase diagram at given T (and p). In terms of the regular solution model it means that the condition T > Ω/2R should be fulfilled. At T = 300 K (see Fig.1) this condition is fulfilled at Ω < 5 kJ/mol. As a result, in Fig.1.d (drawn at Ω = +10 kJ/mol) one can observe curves with a minimum point in their middle ranges and two maximum points at the two ends of the curves, indicating phase separation in the deposited alloy. The corresponding EES diagram can be seen in Fig.2.a (bold line), with phase separation appearing at ΔE = +0.085 mV, where the composition of the cathodic product x jumps from x = 0.98 to x = 0.02. Increasing the temperature to T > Ω/2R, phase separation disappears, as shown by broken line in Fig.2.a with Ω = +10 kJ/mol and T = 1,000 K.

It should be noted that Eq.(2.b) can not be used to calculate the equilibrium situation, when phase separation occurs. As was stated above, Eq-s (2.a, b) can be used only, if only one homogeneous phase can be formed in the given A-B system. Thus, Eq.(2.b) should be used only, if $T > \Omega/2R$.

### *3.1. The EES diagram for a liquid homogeneous Mg-Nd alloy*

Among the papers, published in this special issue [1] only that of Soare et al [1.d] deals with co-deposition of two metals, forming a homogeneous liquid alloy. Experimentally it has been found [1.d] that at the current density of 3.9 A/cm$^2$ at 850 $^o$C from the electrolyte, containing 21 mol% $NdF_3$ + 72 mol% LiF + 7 mol% $MgF_2$ + some $Nd_2(CO_3)_3$, after 6 hours of electrolysis, 61 g of Mg-Nd alloy was obtained with 19.2 w% of Mg, corresponding to $x_{Mg} = 0.58$ [1.d]. Although thermodynamic information on the Mg-Nd system is quite scare, we found that this system can be approximately described with $\Omega \cong -40$ kJ/mol (see data of [10]).

The EES diagram of the $Mg^{+2}$-$Nd^{+3}$ system at 850 $^o$C has been constructed by us using Eq-s (2-3), with $\Omega \cong -40$ kJ/mol (see Fig.3). For the given temperature, this is a unique EES diagram of the $Mg^{+2}$-$Nd^{+3}$ system, i.e. it is valid, regardless the composition of the molten salt. Molten salts with different compositions will provide different $\Delta E$ values, and so, from each particular molten salt, generally different alloy compositions can be synthesized. It should be noted that this EES diagram is principally valid only at infinitely low current density. However, if the actual current density is lower than the diffusion limiting current densities of components, and is also lower at least by one order of magnitude than the exchange current densities of the components, the EES diagram for alloys is probably close to reality. The exchange current density in high temperature molten salts is usually high, and so at a relatively low cathodic current density, applied in [1.d] for the synthesis of Mg-Nd alloys, the EES diagram presented in Fig.3 is probably valid.

Unfortunately there is no information on the separate deposition potentials of Mg and Nd in the applied electrolyte [1.d], so Fig.3 can not be used to estimate the equilibrium alloy composition. However, Fig.3 can be used in the opposite way: from the measured alloy composition ($x_{Mg} = 0.58$ [1.d]) one can find: $E_{Nd} - E_{Mg} \cong -10$ mV (see the vertical dashed line in Fig.3). This value seems to be realistic, as the difference between deposition potentials of the two pure, quasi-liquid fluorides ($NdF_3$ and $MgF_2$) is about –70 mV [11], which obviously shifts towards a somewhat more positive value upon addition of some $Nd_2(CO_3)_3$, as

this compound has been found to provide an electrochemical active form of $Nd^{+3}$ in the melt [1.d]. Thus, Fig.3 and the results of Soare et al [1.d] appear to be in a good agreement, which confirms the reliability of our calculation method, presented above.

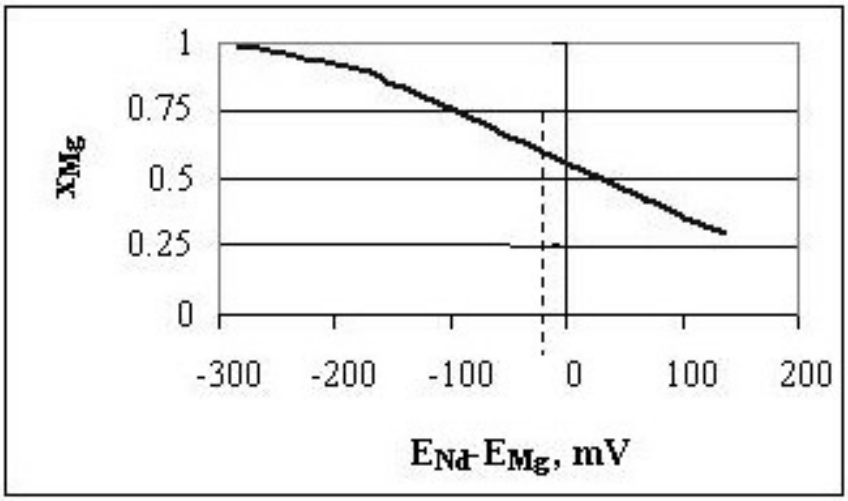


*Figure 3. The EES diagram of the $Mg^{+2}$-$Nd^{+3}$ system at 850 $^{o}$C. The diagram is constructed only in the homogeneous liquid region of the Mg-Nd alloy [10]. The vertical dashed line corresponds to the experimental conditions of Soare et al [1.d].*

## 4. The EES diagram for a system, containing only one compound in the phase diagram

Let us first consider the case, when only one compound $A_pB_q$, with a negligible homogenity range is formed in the A-B system, and it is in equilibrium with practically pure components A and B. In Fig.4, the synthesis potential of the compound, according to Eq.(2) and the deposition potentials of components A and B are drawn as function of parameter ΔE. The compound will be formed as the first cathodic product, if $E_S > E_A$ and if $E_S > E_B$. Substituting these conditions into Eq.(2), the range of ΔE can be found, in which the compound $A_pB_q$ will be the first cathodic product:

$$\Delta E_b = \frac{-\Delta G}{n \cdot x \cdot F} > \Delta E > \frac{\Delta G}{m \cdot (1-x) \cdot F} = \Delta E_a \qquad (4)$$

The 'a' and 'b' points and the intervals of the ΔE values, within which the compound and the two components are formed, are also shown in Fig.4. These intervals are functions of temperature (and pressure) only. Thus, the EES diagrams, previously calculated by the Author [2-6] were constructed in the T - ΔE coordinates, and those EES diagrams are uniquely valid for any ionic liquid or molten salt system of any composition, consisting of some $A^{+n}$ and $B^{+m}$ ions. As the value of ΔE is a difficult function of both composition and temperature, to each particular composition and temperature a 'working point' will correspond on the EES diagrams. Thus, the equilibrium phase at low current densities will be a function of temperature and melt composition only (at least, below 10 MPa).

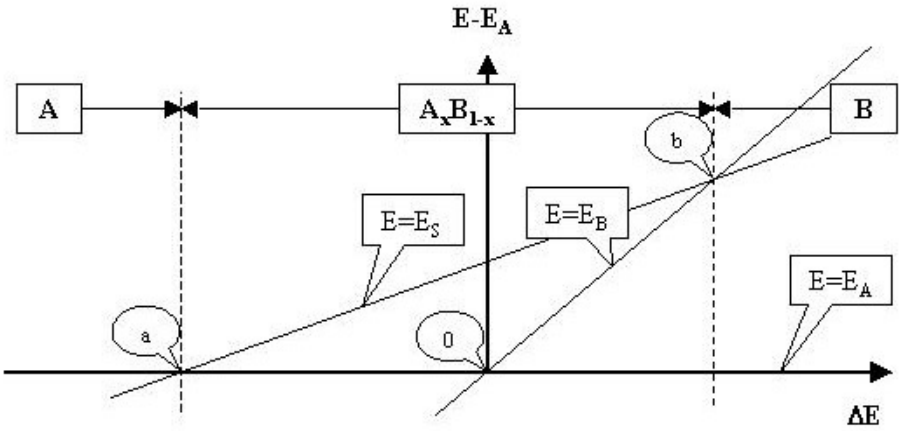


*Figure 4. The relative (to EA) deposition and synthesis potentials (E) as functions of parameter ΔE. The intervals of ΔE values, where phases A, $A_xB_{1-x}$ and B form as first cathodic products, are shown at the top of the figure.*

### *4.1. The EES diagram for a solid Si-C system*

The only paper among those, published in this special issue [1], dealing with a system, in which only one line compound is formed, which is in equilibrium with its practically pure components, is that of Devyatkin [1.l]. In a Si-C system SiC (with practically no homogenity range) is in equilibrium with practically pure C and Si below 1404 °C [12]. As was shown by Devyatkin [1.l], SiC coating on stainless steel cathode can be obtained from $NaCO_3$-$Li_2CO_3$-$SiO_2$ (4 wt%)

melt at 750 $^{o}$C, under $CO_2$ gas atmosphere of 1 bar pressure.

The EES diagram for the $Si^{+4}$-$C^{+4}$ system is shown in Fig.5, calculated by Eq.(4), as function of temperature. The Gibbs energy of formation of SiC has been taken from the compilation [11]. As for this case n = m, and x = 0.5, according to Eq.(4) the phase separation lines will be symmetrical, i.e. at each temperature: $\Delta E_a = -\Delta E_b$. As one can see from Fig.5, the electrochemical synthesis of SiC as first cathodic product is possible at 750 $^{o}$C, if the deposition potentials of Si and C are closer to each other than 170 mV.

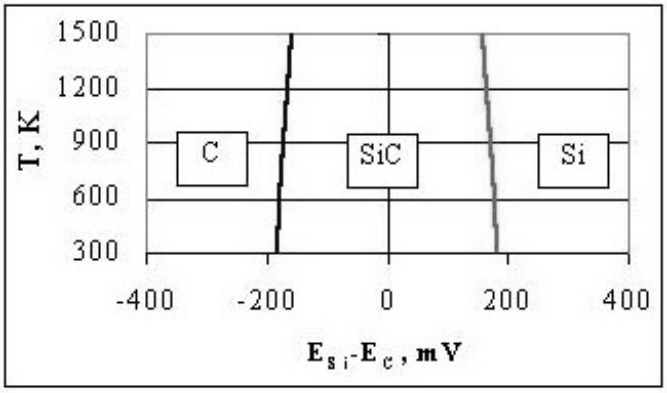


*Figure 5. The EES diagram of the $Si^{+4}$-$C^{+4}$ system showing stability ranges of C and Si deposition, and SiC electrochemical synthesis as first cathodic products.*

According to experiments [1.l], this was not the case, as carbon was deposited at a much more positive potential than Si. Nevertheless, SiC was actually obtained during the galvanostatic electrolysis of the above mentioned system, at least, above 700 $^{o}$C [1.l]. In fact, at low current densities only C can be deposited, being soluble in the cathode material. Above its diffusion limiting current density, SiC will become a stable product. Its stoichiometry is ensured in a certain range of current densities, as the surplus carbon can be dissolved in the cathode material (that might be the reason that below 700 $^{o}$C, when diffusion of C into steel was very much limited, no synthesis was observed). The second reason, why the synthesis of a stoichiometric compound appeared to be possible outside the range, indicated in Fig.5, is that the only compound in the Si-C phase

diagram is SiC, having practically no homogenity range and no solubility in C [12].

### *4.2. The EES diagrams for some III-V semiconducting systems*

Among all possible binary systems, containing a single compound with practically no homogenity range and no solubility in its components' phases the majority of the systems are non-transitional metal – non-transitional metal systems. Among them, there is a particular interest in synthesizing A(III)-B(V) semiconductor compounds (A = Al, Ga, In, B = As, Sb) from ionic liquids [13]. Cations, $Al^{+3}$, $Ga^{+3}$, $Ga^{+}$, $In^{+3}$ and $In^{+}$ from one hand, and cations $As^{+3}$, $Sb^{+3}$ from the other hand have relatively stable chloride compounds, which in principle can be dissolved in different ionic liquids and can be used to synthesize AlAs, AlSb, GaAs, GaSb, InAs and InSb.

When m = n = 3 and x = 0.5 for all these compounds, from Eq.(4): $\Delta E_a = -\Delta E_b$. This maximum potential difference, allowing the formation of the A(III)B(V) compounds as first cathodic product are calculated in Table 1.a. The maximum temperature in Table 1.a is selected to ensure negligible solubility of the compound in any of its components, according to the phase diagram [12]. For comparison, in the last row of Table 1.a the difference in deposition potentials between B and A from imaginary liquid, pure $BCl_3$ and $ACl_3$ compounds are given, according to [11]. One can see that this difference is always much larger than the interval of stable synthesis of the A(III)B(V) compound. Thus, the electrochemical synthesis of the A(III)B(V) compound seems to be feasible only if special complex chemistry is involved in order to shift the two potentials towards each other. However, if the $As^{+3}$ or $Sb^{+3}$ ions are kept at low concentrations in the melt, above their diffusion limiting current densities the synthesis of different one-phase A(III)B(V) compounds are possible, if one conducts the electrolysis at controlled potential, in the excess of $Al^{+3}$, $Ga^{+3}$ and $In^{+3}$ ions.

Particularly, the synthesis of AlAs and AlSb compounds seems to be feasible from room temperature chloro-aluminate ionic liquids. The electrolysis should be performed in a potentiostatic way at a certain potential range, being more positive than 398 mV (or somewhat less) for AlAs and by 165 mV (or somewhat less) for AlSb compared to the deposition potential of bulk aluminum (for the potentials see Table 1.a). It should be mentioned that alloys of different compositions were obtained from low temperature chloro-aluminate melts in a similar way in the Al-Ag, Al-Au, Al-Co, Al-Cu, Al-Fe, Al-Ni systems [9]. A well

defined cathodic product could not be obtained in these systems, because there are several compounds forming in all of them [12], in contrast to the Al-As and Al-Sb phase diagrams [12].

*Table 1.a. The synthesis intervals of different A(III)-B(V) compounds from $A^{+3}$ and $B^{+3}$ ions*

| Compound A(III)-B(V) | T, K | $-\Delta E_a=\Delta E_b$. , mV | $E^o_{B(V)}-E^o_{A(III)}$, mV |
|---|---|---|---|
| AlAs | 300 | 398 | 1,240 |
| | 900 | 383 | - |
| AlSb | 300 | 165 | 1,020 |
| | 900 | 140 | - |
| GaAs | 300 | 243 | 660 |
| | 800 | 185 | - |
| GaSb | 300 | 133 | 450 |
| | 600 | 92 | - |
| InAs | 300 | 180 | 620 |
| | 700 | 149 | - |
| InSb | 300 | 88 | 410 |
| | 400 | 82 | - |

Compounds GaAs, GaSb, InAs and InSb can be probably also synthesized from some ionic liquids, containing a small (controlled) amount of $As^{+3}$ or $Sb^{+3}$ ions and the excess amount of $Ga^{+3}$ or $In^{+3}$ ions. The synthesis should be performed at a potential, somewhat more positive than that of the bulk deposition potential of Ga and In, by a value, somewhat less than that, indicated in Table 1.a for $\Delta E_a$. However, for such a potentiostatic synthesis, a stable reference electrode

is requested to control the process. It should also be mentioned that during co-deposition from low temperature ionic liquids, sometimes instead of equilibrium phases some non-equilibrium phases are formed (see for example [1.a]).

In addition to $A^{+3}$ ions, also $A^{+}$ ions are stable in ionic liquids, their relative stability increasing in the row: Al → Ga → In → Tl. The results of calculations, with $Ga^{+}$ and $In^{+}$, being the electrochemical active species (i.e. n = 1), are shown in Table 1.b. As one can see from comparison of Tables 1.a-b, if $Ga^{+}$ and $In^{+}$ are the electrochemical active species, the one-step formation of GaAs, GaSb, InAs and InSb compounds become more realistic for two reasons:

i. the $\Delta E_b$ value increased by 3 times, compared to the case for $Ga^{+3}$ and $In^{+3}$,
ii. the deposition potentials of $As^{+3}$ and $Sb^{+3}$ can be shifted by some complex formation to a more negative side in a more selectively way due to the charge difference between ions (m > n), without changing the potentials of $Ga^{+}$ and $In^{+}$, what is less realistic for the m = n case, i.e. without changing the potentials of $Ga^{+3}$ and $In^{+3}$.

From the evaluated difference of standard potentials (see last row of Table 1.b), the one-step co-deposition of GaSb seems to be most realistic (among those, considered) from an ionic liquid, containing $Ga^{+}$ and $As^{+3}$ ions, if the $As^{+3}$ ions are selectively complexed by an anion.

## 5. The EES diagram for a system, containing several compounds in the phase diagram

If there are several stable compounds in the A-B phase diagram, Eq.(2) should be applied to all of them, and a figure, similar to Fig.4 should be constructed, with all the compounds to be characterized by a straight line. The first cathodic product will be again the one, having the most positive synthesis potential. If appropriate thermodynamic values are used, it always will turn out that a certain interval of parameter ΔE will correspond to each stable compound, at which this particular compound has a most stable synthesis potential, and thus it will be the equilibrium cathodic product. The sequence of stable phases as function of parameter ΔE will be the same as that in the corresponding phase diagram. Thus, for example in the Al-Ti EES diagram the phases at room temperature will be positioned in the following sequence: Al – $Al_3Ti$ – $Al_2Ti$ – AlTi - $AlTi_3$ – Ti [12].

*Table 1.b. The synthesis intervals of different A(III)-B(V) compounds from $A^+$ and $B^{+3}$ ions*

| Compound A(III)-B(V) | T, K | $\Delta E_a$, mV | $\Delta E_b$, mV | $E^o_{B(V)}-E^o_{A(III)}$, mV |
|---|---|---|---|---|
| AlAs | 300 | -398 | 1,194 | - |
| | 900 | -383 | 1,149 | - |
| AlSb | 300 | -165 | 495 | - |
| | 900 | -140 | 420 | - |
| GaAs | 300 | -243 | 729 | (<660)* |
| | 800 | -185 | 555 | - |
| GaSb | 300 | -133 | 399 | (<450)* |
| | 600 | -92 | 276 | - |
| InAs | 300 | -180 | 540 | 734 |
| | 700 | -149 | 447 | - |
| InSb | 300 | -88 | 264 | 521 |
| | 400 | -82 | 246 | - |

** Estimated from the condition that liquid GaCl is somewhat less stable than liquid $GaCl_3$*

The potential, dividing the stability regions of Al and $Al_3Ti$ on one hand, and regions of $AlTi_3$ and Ti, on the other hand, can be calculated by Eq.(4). For other phase boundaries the competition of different compounds should be taken into account.

Let us consider compound phases 1 and 2, following each other in the phase diagram, denoted by compositions x1 and x2, and thus characterized by different values of c1 and c2, and also by different formation energies $\Delta G1$ and $\Delta G2$. Then, compound 2 will become more stable than compound 1, if $E_{s2} > E_{s1}$. Substituting Eq.(2) into this condition, the following condition can be derived for

stability of compound 2, relative to compound 1:

$$\Delta E > \frac{c1 \cdot \Delta G2 - c2 \cdot \Delta G1}{m \cdot F \cdot \left[c1 \cdot (1 - x2) - c2 \cdot (1 - x1)\right]} \tag{5}$$

Eq. (5) can be considered as a generalized version of Eq.(4). Using Eq-s (4, 5), stability ranges for all stable compounds can be calculated at given temperature. Repeating this procedure for several temperatures, EES diagrams can be constructed.

### *5.1. The EES diagram for the Al-Ti system*

There is more than one compound is formed in the phase diagram of the majority of systems, studied in this special issue [1]. As in our previous papers mainly boride systems were studied [2-7], let us use Eq-s (4-5) for the Ti-Al system, as an example of systems with numerous possible phases. Electrochemical synthesis of Ti-Al phases has been studied by Stafford et al [1.b, 14] at 150 $^{o}$C in a chloro-aluminate melt with controlled additions of $TiCl_2$. The apparent limit of maximum 28 at % Ti in the synthesized alloys was found, which did not increase further with increasing the $TiCl_2$-content of the melt. This phenomenon was explained by supposing that Ti-deposition appears from electrochemically active $[Ti(AlCl_4)_3]^-$ anions [1.b], leading to the theoretical maximum of 25 at% Ti in the alloy.

Thermodynamic properties of the Ti-Al system are known with relatively high certainty only for TiAl and $TiAl_3$ phases [11]. Thermodynamic properties of the two other phases (see Table 2) have been estimated by us using the Ti-Al phase diagram [12]. The results of our calculations, performed by Eq-s (4-5) are presented in Table 2 and Fig.6. From Table 2 and Fig.6 one can see that the compound $Al_3Ti$ has an exceptionally wide stability range in the EES diagram, compared to other Al-transitional metal systems, studied previously from the same chloro-aluminate melts [9]. Such a wide electrochemical window of the formation of the $Al_3Ti$ intermetallic can serve as an alternative explanation to the apparent limit of Ti-content in Al-Ti deposits, established experimentally in [1.b, 14].

*Table 2. Stable potential intervals of synthesis of different phases in the $Al^{+3}$-$Ti^{+2}$ system*

| Phase | x | c | T<br>K | ΔG<br>kJ/g-atom | $\Delta E_1=E_{Ti}-E_{Al}$<br>mV | $\Delta E_2=E_{Ti}-E_{Al}$<br>mV |
|---|---|---|---|---|---|---|
| Al | 1 | 3 | 300 | 0 | -∞ | -723 |
| | | | 1000 | 0 | -∞ | -626 |
| $Al_3Ti$ | 0.75 | 2.75 | 300 | -34.870 | -723 | -128 |
| | | | 1000 | -30.199 | -626 | -172 |
| $Al_2Ti$ | 0.666 | 2.666 | 300 | -36.05 | -128 | -79 |
| | | | 1000 | -32.30 | -172 | -105 |
| AlTi | 0.5 | 2.5 | 300 | -36.646 | -79 | +110 |
| | | | 1000 | -34.093 | -105 | +71 |
| $AlTi_3$ | 0.25 | 2.25 | 300 | -26.6 | +110 | +368 |
| | | | 1000 | -23.6 | +71 | +326 |
| Ti | 0 | 2 | 300 | 0 | +368 | +∞ |
| | | | 1000 | 0 | +326 | +∞ |

### *5.2. The Al-rich side of the ES diagram for the Al-Ti system*

In this paper, so far only EES diagrams have been calculated, being valid in principle only at zero current density. Practically these diagrams are valid, if the actual current density is much lower than the exchange current density of the components. Unfortunately we have no information on the exchange current densities of Al and Ti in chloro-aluminate melts, as function of $TiCl_2$ content and

temperature. If those values were known, the non-equilibrium ES diagram could be calculated at a fixed temperature, in coordinates ΔE – logi (where i is the current density) [7].

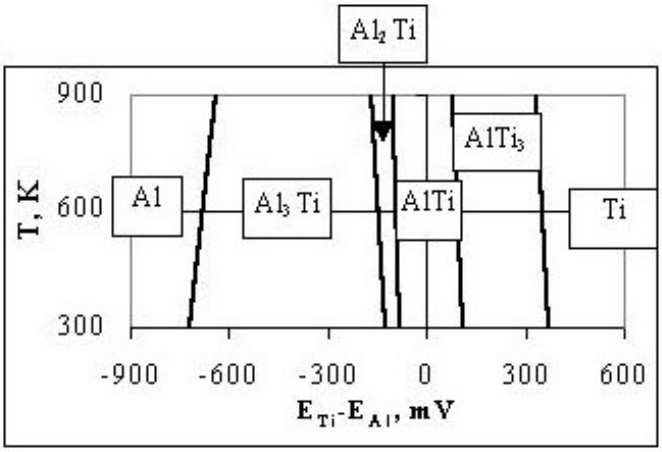


*Figure 6. The Equilibrium Electrochemical Synthesis Diagram of the $Al^{+3}$-$Ti^{+2}$ system.*

Nevertheless, such an ES diagram can be constructed semi-schematically for the Al-rich side of the Al-Ti diagram at 150 °C (see Fig.7), based on the principle, developed earlier [7]. The vertical lines in the ES diagram correspond to the equilibrium ΔE values of phase transitions in the EES diagram, between phases Al – $Al_3Ti$ and $Al_3Ti$ – $Al_2Ti$ at 150 °C (see Fig.6). The line, drawn at a slope, separating the 1-phase $Al_3Ti$ region from the 2-phase (Al + $Al_3Ti$) region is due to the charge transfer limitations of Ti deposition at high depolarizations of Ti-deposition. The logarithm of this "exchange limiting current density" ($i_{lim}$) is a linear function of parameter ΔE [7]. Parameter $i_{lim}$ increases when the exchange current density of Ti deposition increases, which does so with increasing the $TiCl_2$ content of the melt. Thus the line, separating the 1-phase $Al_3Ti$ region from the 2-phase (Al + $Al_3Ti$) region will be shifting towards higher current density values with increasing the $TiCl_2$ content of the melt.

The circle in Fig-s. 7.a-c represents the working point (composition, current density), corresponding to a given electrochemical synthesis experiment, conducted in a galvanostatic way. When the $TiCl_2$ content of the melt increases, this working point will be shifting gradually to more and more positive ΔE

7.a.

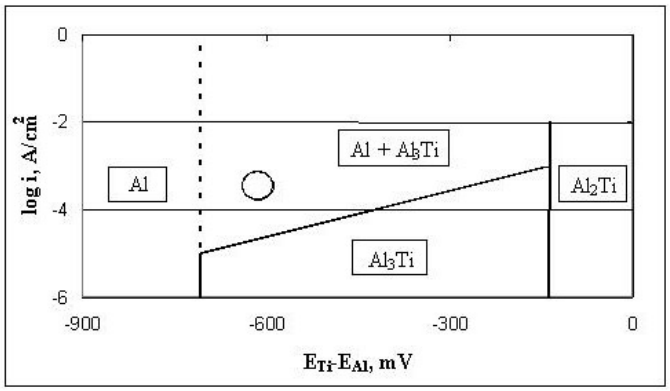


7.b.

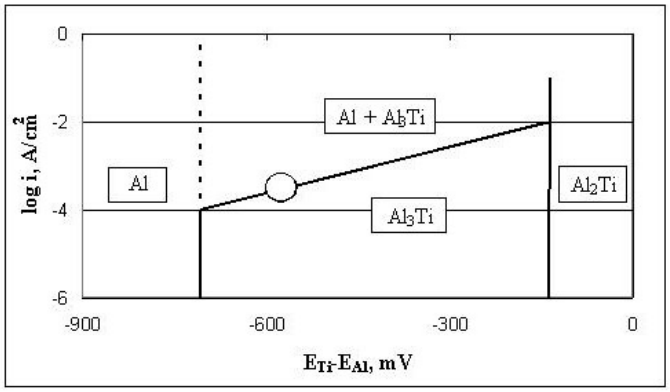


7.c.

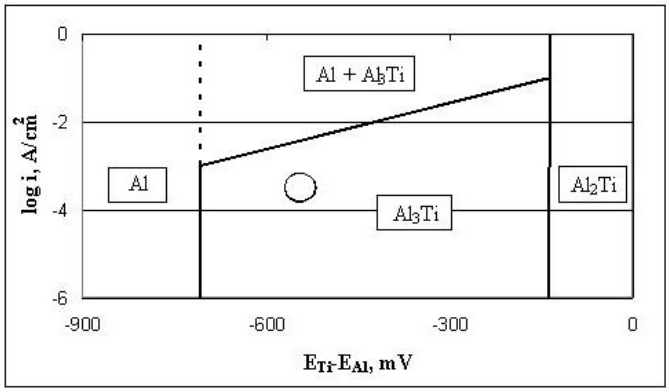


*Figure 7. The Al-rich part of the non-equilibrium ES diagram for the $Al^{+3}$-$Ti^{+2}$ system at 150 $^{o}$C as function of logarithm of the cathodic current density (semi-schematic). From Fig. 7.a to Fig. 7.c the $Ti^{+2}$ content of the melt gradually increases.*

values, according to the Nernst equation. However, as the stability range of the $Al_3Ti$ is very wide (about 600 mV – see Fig-s 6-7), and the deposition potential shift of Ti is only 42 mV per one order of magnitude concentration of $TiCl_2$, this working point will much probably remain inside the $Al_3Ti$ stability interval, whatever is the $TiCl_2$ content of the melt (supposing that Al is considerably more electrpositive in chloroaluminate melts compared to Ti, what is probably the case) [1.b, 14]. In Fig-s 7.a-c, the situation, corrersponding to three different experiments are characterized. All these experiments are conducted with the same cathodic current density, in electrolytes, having higher and higher $TiCl_2$ content. One can see that by increasing the $TiCl_2$ content, the line, separating the 1-phase $Al_3Ti$ region from the 2-phase ($Al + Al_3Ti$) region shifts through the working point. Thus, at low $TiCl_2$ content (Fig. 7.a) the cathodic product is Al with some $Al_3Ti$, for medium $TiCl_2$ content (Fig.7.b) the cathodic product is already a practically pure $Al_3Ti$ phase, which does not change with further increase of the $TiCl_2$ content of the melt (Fig.7.c).

The average Ti-content (in atomic fraction) of the two-phase ($Al + Al_3Ti$) cathodic product can be calculated from the following equation:

$$x_{Ti} = \frac{3}{1 + 11 \cdot \frac{i}{i_{\lim}}} \tag{6}$$

where i and $i_{lim}$ is the actual current density of electrolysis and the exchange limiting current density of phase separation between ($Al_3Ti$) and ($Al + Al_3Ti$) regions, at the $\Delta E$ value, corresponding to the given electrolyte composition. Eq.(6) should be used only at $i = i_{lim}$, providing $x_{Ti} = 0.25$.

Analysing Eq.(6) one can make the following qualitative conclusions:

i. if the $TiCl_2$ content of the melt, and thus the value of $i_{lim}$ is fixed, the Ti-content of the cathodic product will be decreasing if the actual current density of electrolysis is increased,
ii. if he current density is fixed, the Ti-content of the cathodic product will be increasing (up to maximum 25 at %), if the $TiCl_2$ content of the melt, and thus the value of $i_{lim}$ is increased.

The above conclusions are in good qualitative agreement with experimental

results of Stafford et al [1.b, 14], especially at high rotation speeds of the electrode, i.e. when diffusion limitations of $Ti^{+2}$ ions in the electrolyte are overcome. This condition is important, as in the above simplified model only charge transfer limitations are taken into account (see [7] for diffusion limitations). In order to make the non-equilibrium ES diagram of the $Al^{+3}$ – $Ti^{+2}$ system more realistic, exchange current densities and diffusion limiting current densities of the components should be measured or modeled as function of electrolyte composition and temperature.

## 6. Conclusions

The principle of equilibrium electrochemical synthesis diagrams, introduced by the author for stoichiometric phases earlier, has been extended to homogeneous alloys in this paper. As an example, the EES diagram of the liquid Gd-Mg system has been constructed. For systems with compound formation, EES diagrams for the Si-C system, for some A(III)-B(V) ystems, and for the Ti-Al systems have been constructed. These diagrams can be used for better interpretation of experimental results and for further improvement of technologies of producing alloys and compounds by electrochemical synthesis from ionic liquids and molten salts.

## Acknowledgements

The author is grateful to G.R.Stafford (NIST, USA) and to F.Endres (Technical University of Clausthal, Germany) for valuable discussions.

## Literature

1. in JMM B, 2003 - see in this special issue:
   1.a. T.Tsuda, C.L.Hussey (Al-V alloys),
   1.b. G.R.Stafford (Al-Ti alloys),
   1.c. P.Taxil, P.Chamelot, L.Massot, C.Hamel (Ni-Ta, Ni-Nd alloys and Ta-carbides),
   1.d. V.Soare, M.Burada, T.Ostvold, C.Kontoyannis, E.Stefanidiki (Mg-Nd alloys),
   1.e. Y.Ito, T.Nishikiori (nitrides, hydrides, Ni-Y, Zr-Al alloys),
   1.f. G.A.Bukatova, S.A.Kuznetsov, M.Gaune-Escard (Eu borides),

1.g. O.V.Makarova, et al. (Ta borides),
1.h. R.Krendelsberger et al. ($TiB_2$),
1.i. Kh.B.Khushkhov et al. (La-Gd borides),
1.j. I.A.Novoselova, S.V.Volkov, N.F.Oliinyk, V.I.Shapoval (carbides),
1.k. A.I.Anfinogenov, Z.S.Martemyanova (Ti-Si-C compounds),
1.l. S.V.Devyatkin (SiC and Ti-Si, B-Si, Ti-Si-B compounds).
2. G.Kaptay, E.Buzinkay, Molten Salts Forum, 5-6**,** 359 (1998)
3. G.Kaptay, E.Berecz, Chapter 11 in: „Chemical Thermodynamics - A 'Chemistry for the 21st Century' monograph", ed. T. Letcher, Blackwell Science, 135 (1999)
4. G.Kaptay, S.A.Kuznetsov, Plasmas & Ions, 2, 45 (1999)
5. G.Kaptay, in: „Advances in Molten Salts – From Structural Aspects to Waste Processing", ed. by M.Gaune-Escard, begell house inc., NY, 249 (1999)
6. H.B.Kushov, G.Kaptay, A.S.Uzdenova, M.K.Vinidzheva: Rasplavi, 2002, No.1, pp.44-48.
7. G.Kaptay – paper submitted to Proceedings of the Electrochemical Society, May 2002
8. A.Brenner: Electrodeposition of Alloys, vol.1, 1963, Academic Press, New York.
9. G.R.Stafford, C.L.Hussey: in "Advances in Electrochemistry Science and Engineering", ed. by R.Alkire and D.Kolb, 2002, Wiley-VCH, Weinheim, Germany, p.275
10. R.Hultgren, P.D.Desai, D.T.Hawkins, M.Gleiser, K.K.Kelley: Selected Values of Thermodynamic Properties of Binary Alloys - AMS, Materials Park, Ohio, 1973.
11. I.Barin: Thermochemical Properties of Pure Substances, VCh, 1993, in 2 parts
12. T.B.Massalski (ed): Binary Alloy Phase Diagrams, second ed., 3 volumes, ASM International, 1990.
13. F.Endres – private communication (Technical University of Clausthal, Germany, http://www.imet.tu-clausthal.de/agfe)
14. T.Tsuda, C.L.Hussey, G.R.Stafford, J.E.Bonevich – JES, 2003, vol.150 (4), C234-C243